J Mater Sci

Composites & nanocomposites

Nanoparticle-based impregnation coatings for wood: improving hydrophobicity, mechanical properties, and blue stain fungi resistance through structure–property relationship

Dabosmita Paul[1,*], Miha Humar[2], Daniela Tesařová[1], Marko Petrič[2], and Milan Gaff[1,3]

[1] *Department of Furniture, Design and Habitat (FFWT), Mendel University in Brno, 1, Zemědělská 1665, Černá Pole, 613 00 Brno-sever, Czech Republic*

[2] *Biotechnical Faculty, Department of Wood Science and Technology, University of Ljubljana, Jamnikarjeva 101, 1000 Ljubljana, Slovenia*

[3] *Faculty of Civil Engineering, Czech Technical University in Prague, Experimental Centre, Prague, Czech Republic*

Received: 5 May 2025
Accepted: 15 July 2025

ABSTRACT

Wood is an organic material that is highly susceptible to moisture, which compromises its performance, accelerates decay, and promotes mould growth, thereby reducing its service life. This study presents a comparative assessment of cost-effective solutions for enhancing the hydrophobicity, mechanical properties, and blue-stain resistance of wood surfaces by evaluating the effects of silicon dioxide (SiO_2), zinc oxide (ZnO), and titanium dioxide (TiO_2) particle coatings on Scots pine wood. Low-concentration particles were applied via an impregnation coating method, resulting in the formation of a nanocomposite between the wood and the particles. The coated and uncoated samples were then exposed to blue-stain fungi. To further analyse the effects, the exposed samples were characterised using scanning electron microscopy (SEM) to analyse particle morphology and observe fungal colonisation, and energy-dispersive X-ray spectroscopy (EDS) to determine elemental distribution. Fourier-transform infrared spectroscopy (FTIR) was used to confirm interactions between the nanoparticles and wood components. Mechanical and physical tests were conducted to evaluate the durability and resistance of the coated wood against blue-stain fungi. The results showed a significant improvement in surface hydrophobicity following coating application, which remained stable even after exposure to fungi. Moreover, distinct differences in fungal resistance were observed among the nanoparticle types, with ZnO showing the highest effectiveness. A new approach was also introduced to assess the mechanical performance of the coatings. This study offers insight into nanoparticle coatings as a sustainable strategy for enhancing wood surfaces in construction and outdoor furniture applications.

Handling Editor: Chris Cornelius.

Address correspondence to E-mail: dabosmita.paul@mendelu.cz

E-mail Addresses: miha.humar@bf.uni-lj.si; daniela.tesarova@mendelu.cz; marko.petric@bf.uni-lj.si; milan.gaff@mendelu.cz

https://doi.org/10.1007/s10853-025-11247-0

Published online: 31 July 2025

Springer

GRAPHICAL ABSTRACT

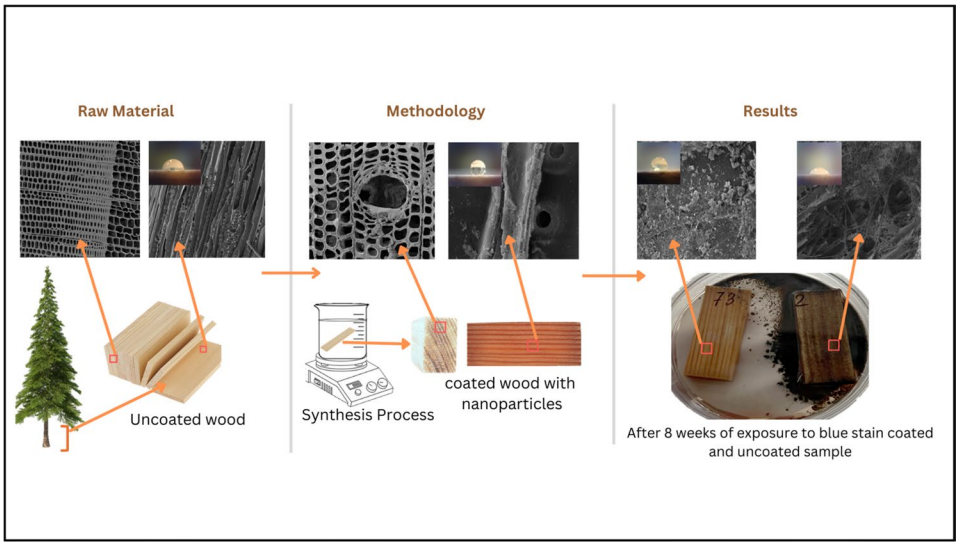

Introduction

Wood has long been in furniture and construction applications and is regaining importance due to the increasing focus on climate change mitigation [1]. As a renewable and biodegradable material, wood is primarily composed of cellulose, hemicellulose, and lignin [2, 3] yet remains highly vulnerable to abiotic stressors such as moisture, ultraviolet (UV) radiation, and temperature fluctuations, as well as biotic factors including fungi and insects. These agents contribute to degradation, discolouration, and a decline in mechanical strength, significantly reducing the service life of wood-based materials in outdoor use compared to alternative building options [4].

Furthermore, moisture significantly increases wood's susceptibility to fungal colonisation, with blue-stain fungi and mould being particularly problematic. These fungi cause blue, grey, or black streaks on the sapwood [5]. They affect both softwoods and hardwoods, including roundwood, sawn timber, and finished products. Feeding on nutrients in parenchyma cells, they secrete enzymes and degrade bordered pits, increasing permeability and vulnerability to further decay [6]. While they do not compromise dimensional quality, they reduce aesthetics and commercial value, especially in outdoor applications [6]. Therefore, further development of wood properties is important in advancing material science.

One way to address this issue is by reducing wood's moisture absorption and hygroscopicity, thereby preventing biological deterioration. Conventional wood protection methods [7], including acetylation [8], furfurylation [9], DMDHEU [10], and heat treatment [11], as well as surface coatings such as paint and varnish, have been developed to enhance wood durability [12]. Although these methods have their advantages, only a few have been used in industry [13]. However, these approaches often present limitations, such as high costs, reduced effectiveness over time, and environmental concerns [14, 15]. Consequently, their protective effectiveness diminishes over time, requiring regular maintenance or reapplication to ensure continued performance in outdoor environments [16].

Recent advancements in nanotechnology offer promising alternatives [17]. Oxide nanoparticles such as silicon dioxide (SiO_2), zinc oxide (ZnO), and titanium dioxide (TiO_2) [9, 18, 19] are being investigated for their high surface area, chemical stability, and ability to bond with wood's hydroxyl groups [20]. Due to their nanoscale dimensions, they can penetrate the pores of wood and reinforce the material's internal structure, resulting in more durable protective systems [21]. These characteristics enable nanoparticles to enhance hydrophobicity, UV

resistance, mechanical strength, and biological resistance through the formation of organic–inorganic hybrid composites [22, 23].

This study aimed to evaluate and compare the effectiveness of Scots pine sapwood coatings incorporating silicon dioxide, zinc oxide, and titanium dioxide in resisting blue-stain fungal colonisation. Nanoparticles were synthesised and deposited using a bottom-up impregnation method, allowing integration into both the wood surface and matrix [17, 24, 25]. Importantly, low concentrations of nanoparticles were used to minimise potential toxicity while maintaining performance. Scots pine was selected for its high sapwood content, which is particularly susceptible to blue-stain fungi [26], as well as its availability and uniform properties, making it a standard species for durability testing [27, 28]. The resulting coated wood, which combines natural fibres with inorganic nanoparticles, forms a wood-based nanocomposite hybrid material [29] designed to enhance protection and mechanical resilience against blue stain fungi. Recent research has focused on nanomaterials in saturation coatings to develop durable, cost-effective wood protection. However, few studies compare their effectiveness against blue-stain fungi. This study addresses that gap by evaluating wettability and mechanical properties post-exposure. While crystallinity was not assessed, it is a target for future research, as it lay beyond the current study's scope.

This study aligns with green nanotechnology [30] by using low concentrations of biocompatible nanoparticles (SiO_2, ZnO, TiO_2) [31] to enhance wood protection while minimising environmental impact. Although generally safe, concerns about potential leaching into soil and water highlight the need for long-term assessments [32]. The novelty of our approach lies in assessing the persistence and functional performance of oxide nanoparticles following exposure to blue-stain fungi. We conducted a comparative analysis using equal concentrations of SiO_2, ZnO, and TiO_2 to determine which nanoparticles remained most effective after exposure to fungi. The comparative result provides a practical and sustainable strategy for developing environmentally friendly wood protection systems, with an emphasis on long-term stability and antifungal efficacy under realistic conditions. Our approach supports sustainable material science by reducing chemical use and promoting eco-conscious alternatives.

Materials and methods

Materials

Scots pine wood samples were prepared in the Mendel University workshop. The chemicals for synthesis were sourced from Thermo Scientific Chemicals and Lach:Ner. Tetraethyl orthosilicate (98%) and titanium (IV) n-butoxide (99 + %) were purchased from Thermo Scientific Chemicals, while ammonium hydroxide (28–30%), sodium hydroxide (≥ 99%), zinc nitrate dihydrate (≥ 99%), and ethanol (99%) were obtained from Lach:Ner. All the chemicals were used without further purification.

Methods

The Scots pine wooden samples were cut into (5 mm × 20 mm × 50 mm) dimensions. The samples were then surface finished with sandpaper. After that, the cut samples were thoroughly washed by ultrasonication in deionised water for 15 min at room temperature (23 °C) and dried at 105 °C in a humidity chamber until their mass remained consistent. Before modification, all the selected samples were placed in the vacuum chamber to clean the dirt from the wood lumen area. All the samples were coated using the impregnation method (bottom-up) [17, 32], and subsequently, both the coated and uncoated samples were exposed to blue stain fungi for eight weeks.

Preparation of SiO_2 nanoparticles coated wood

SiO_2 precursor, tetraethyl orthosilicate (TEOS) 0.5 M, was dissolved in 300 mL of ethanol. The samples were then immersed in this TEOS solution for 1 h. A hydrolysis solution was prepared separately by combining 200 mL of ethanol with 0.2 M ammonium hydroxide (NH_4OH). The hydrolysis solution was gradually added to the mixture, which was stirred vigorously for 2 h. The samples were then left at room temperature (23 °C) for 24 h under constant shaking at 50–100 min^{-1}. Afterwards, the wood samples were removed from the solution and rinsed with deionised water. The samples were first dried at 60 °C for 12 h, then cured at 120 °C for 1 h to set the SiO_2 impregnation in the wood.

Preparation of ZnO nanoparticles coated wood

A 0.5 M solution of zinc nitrate dihydrate was prepared by dissolving the precursor in 300 mL of ethanol under stirring. The samples were then immersed in the zinc nitrate dihydrate solution. After 1 h, a sodium hydroxide solution was added dropwise to the mixture, and the samples were left in the solution at room temperature (23 °C) for 24 h, with constant shaking at 50–100 min^{-1}. After this period, the samples were removed from the solution, washed with distilled water and ethanol. Subsequently, the samples were dried in a drying chamber at 60 °C for 12 h, and then the ZnO-impregnated coating samples were cured at 120 °C for 1 h.

Preparation of TiO_2 nanoparticles coated wood

To prepare a 0.5 M TiO_2 precursor solution, titanium (IV) n-butoxide was dissolved in 300 mL of ethanol under continuous stirring to ensure complete homogenisation. The samples were then immersed in this titanium (IV) n-butoxide solution for 1 h. Another solution was prepared separately by combining 200 mL of deionised water with 0.2 M acetic acid. Then the acetic acid solution was gradually added to the mixture under vigorous stirring and maintained at 60 °C for 2 h. The samples were then left at room temperature (23 °C) for 24 h under constant shaking at 50–100 rpm. Afterwards, the wooden samples were removed from the solution, washed with deionised water, and dried at 60 °C for 12 h. Finally, the samples were cured at 120 °C for 1 h.

Coated and uncoated samples were exposed to blue stain.

The uncoated and coated samples were exposed to blue-stain fungi for eight weeks, in accordance with the standard EN 152–1 (1990). The fungal species Aureobasidium pullulans (de Barry) Arnaud (ZIM L060) and Sclerophoma pithyophila (Corda) Hohn (ZIM L070). The fungal isolates originate from the fungal collection of the Biotechnical Faculty, University of Ljubljana and are available to research institutions on demand [33]. Information regarding the origin of the fungal isolates and details about identification are available in the respective catalogue. These two fungal species develop on wooden products that were either painted or left uncoated and exposed to fluctuations in moisture during service, such as wooden façades, window frames, garage doors, and garden furniture. These two fungi are responsible for 75% of the discolouration of timber in service in the temperate zone [34]. Therefore, these fungi serve as an excellent model organism.

Characterisation method

The uncoated samples, both with and without exposure, as well as the coated samples containing SiO_2, ZnO, and TiO_2, exposed to blue stain, were characterised.

Scanning electron microscopy (SEM) was conducted using the Tescan Mira 3 STAN system to observe the morphologies of particles and fungi on the wood surface. Energy-dispersive X-ray spectroscopy (EDS), performed using the Oxford Instruments AZtecOne system, was employed to analyse the elemental composition and distribution. Before imaging, samples were sputter-coated with a 10 nm gold layer to enhance conductivity. SEM analysis was carried out at an accelerating voltage of 8 kV, enabling high-resolution visualisation of microstructural features and providing detailed insights into nanoparticle interactions with the wood matrix and fungi. Fourier-transform infrared spectroscopy (FTIR) analysis was carried out using an ATR-FTIR setup with a Bruker Invenio S instrument. Each sample was scanned 32 times over a spectral range of 4000–40 cm^{-1} to investigate the bonding interactions between inorganic nanoparticles and the organic components of the wood, as well as to assess the chemical changes in wood properties resulting from exposure to blue-stain fungi. Additionally, mechanical and physical tests assessed durability and resistance to blue staining.

Data analysis

Statistical evaluations were performed using R (R Core Team, 2023). Descriptive statistics were computed with the "dplyr" package [35] to summarise the contact angle data across different coating groups. The analysis included the calculation of sample size (N), mean, standard deviation (SD), standard error (SE), median, interquartile range (IQR), and range (min–max) for each group [36]. The normality of each group was assessed using the Shapiro–Wilk test. The Buchholz hardness and Young's modulus datasets

were found to be non-normally distributed in at least one group; therefore, pairwise comparisons were conducted using the nonparametric Wilcoxon rank-sum test. In contrast, the contact angle data met the normality assumption in all groups ($p > 0.05$). To evaluate the overall effect of nanoparticle treatment on contact angle, a one-way ANOVA was performed, revealing a highly significant difference among groups ($p < 0.001$). Consequently, post hoc analysis was carried out using pairwise two-tailed Student's t-tests between specific group pairs of interest. To control the false discovery rate due to multiple comparisons, p-values were adjusted using the Benjamini–Hochberg method.

Data visualisation was performed using the "ggplot2" package [36].

Results and discussion

Figure 1 illustrates the process of impregnating wood with nanoparticles by leveraging its hierarchical porous structure across multiple scales. Wood, composed of tubular cells with hollow lumens, exhibits a naturally porous architecture at the millimetre, micrometre, and nanometer scales. During the process, wood samples are immersed in a precursor solution containing nanoparticles and kept for 24 h, allowing the solution to penetrate through the lumens and diffuse into the cell walls. At the micrometer scale, nanoparticles infiltrate the wood's internal cellular network, while at the nanometer scale, they interact with the cellulose-rich cell walls. After drying and curing, the nanoparticle-fixed wood cell walls contain hydroxyl (− OH) groups that are capable of forming hydrogen or covalent bonds with the nanoparticles, thereby securing them within the structure [37]. As the solution penetrates the porous wood matrix, the nanoparticles undergo in situ polymerisation, forming nanoparticle–O–nanoparticle (nanoparticles = Zn, Si, Ti) chains that result in a three-dimensional polymeric skeleton with close packing. This interaction facilitates the integration of nanoparticles into the wood matrix through a combination of physical entrapment and chemical bonding, while preserving the original porous structure of the wood [38, 39].

After impregnation, all the coated and uncoated samples were exposed to fungi. Where the samples referred to as Control_A were uncoated and without

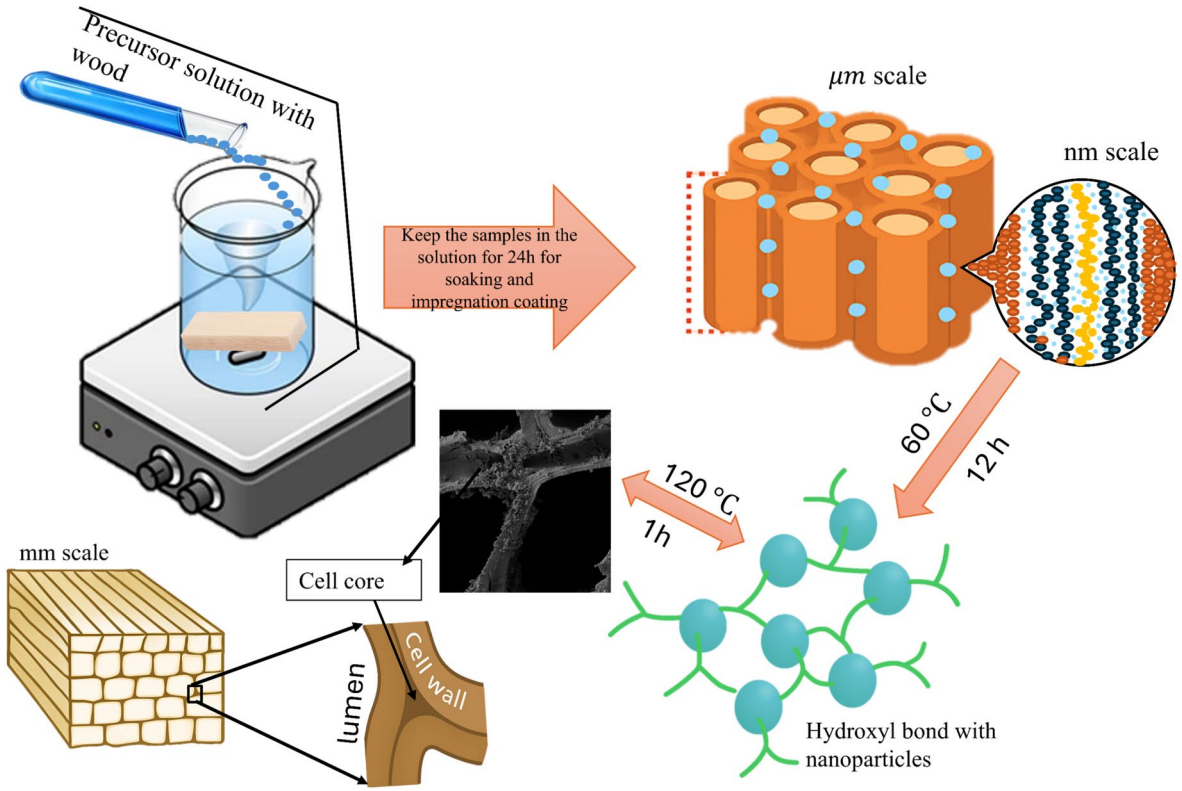

Figure 1 Schematic of experimental set-up for preparing wood-based nanocomposite by impregnation coating.

exposure to blue stain fungi, while Control_B were uncoated and exposed to blue stain. SiO_2, ZnO, and TiO_2 were referred to as wood impregnated with silicon dioxide, zinc oxide, and titanium dioxide nanoparticles and microparticles, and exposed to blue stain fungi. All the samples were compared in the results.

Scanning electron microscopy (SEM)

To gain a deeper insight into the wood's microstructure and the interaction between nanoparticles, blue stain fungi and wood, longitudinal sections of both uncoated and coated samples were examined using SEM.

Figure 2a presents the surface morphology of Control_A samples, revealing a smooth surface with clearly visible pits and aligned wood fibres, characteristic of untreated Scots pine sapwood. In contrast, Fig. 2b shows the Control_B sample, where fungal spores and hyphae extensively colonised the surface. The fungal growth obscures the underlying structure, significantly reducing the visibility of pits and fibres, indicating apparent microbial degradation compared to Control_A.

Figure 3 presents the surface morphology of oxide-coated wood samples (SiO_2, ZnO, and TiO_2) after impregnation and exposure to blue stain fungi. All coated surfaces exhibit greater roughness than the uncoated Control_A sample, indicating successful deposition of oxide materials. In Fig. 3a, the SiO_2-coated sample exhibits a relatively uniform dispersion of spherical particles (yellow arrows), with visible wood fibres and no distinct pit structures. Some signs of blue-stain fungi are present (red circles

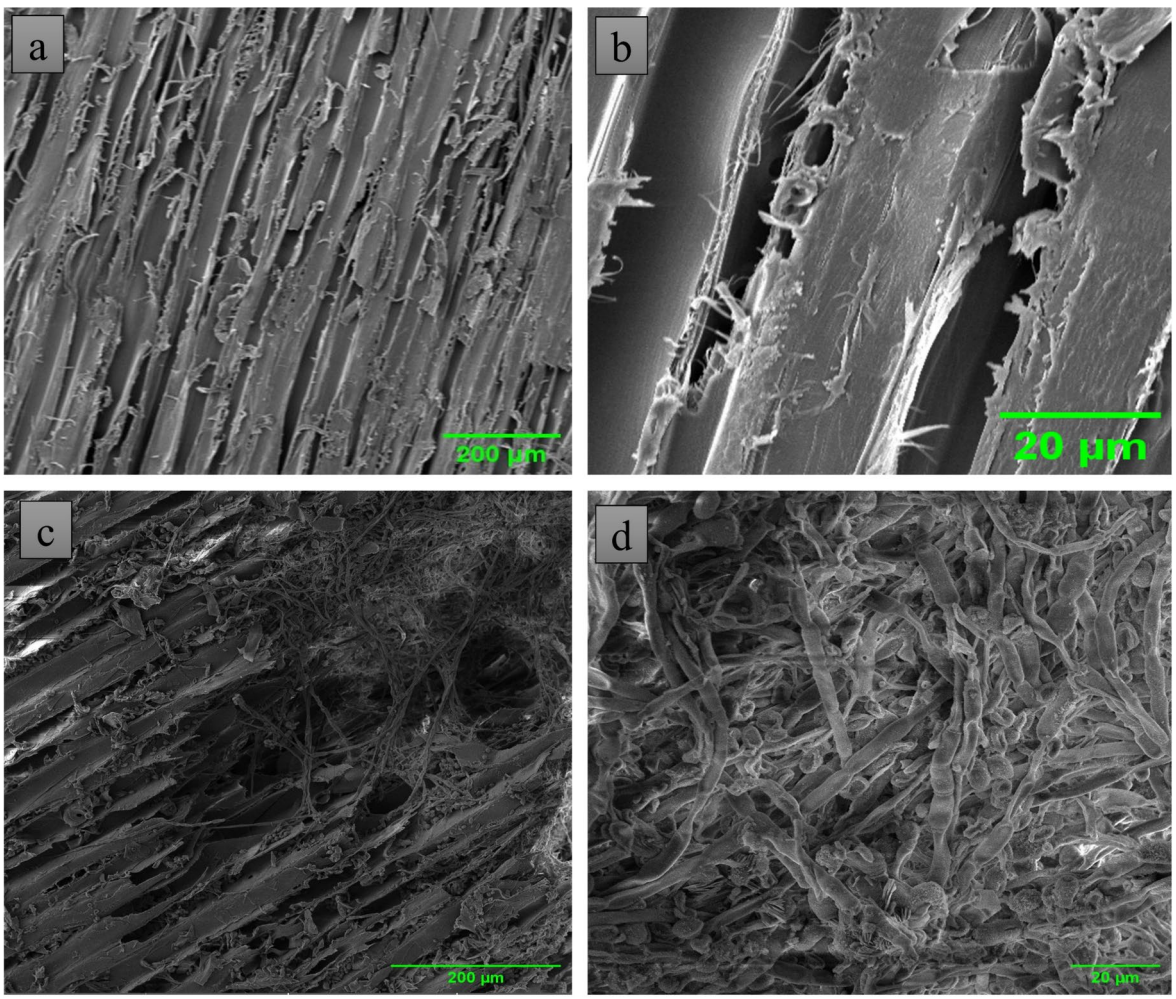

Figure 2 High and low resolution of SEM image: **a** Control_A uncoated and without exposure to blue stain fungi, **b** Control_B uncoated and exposed to blue stain fungi.

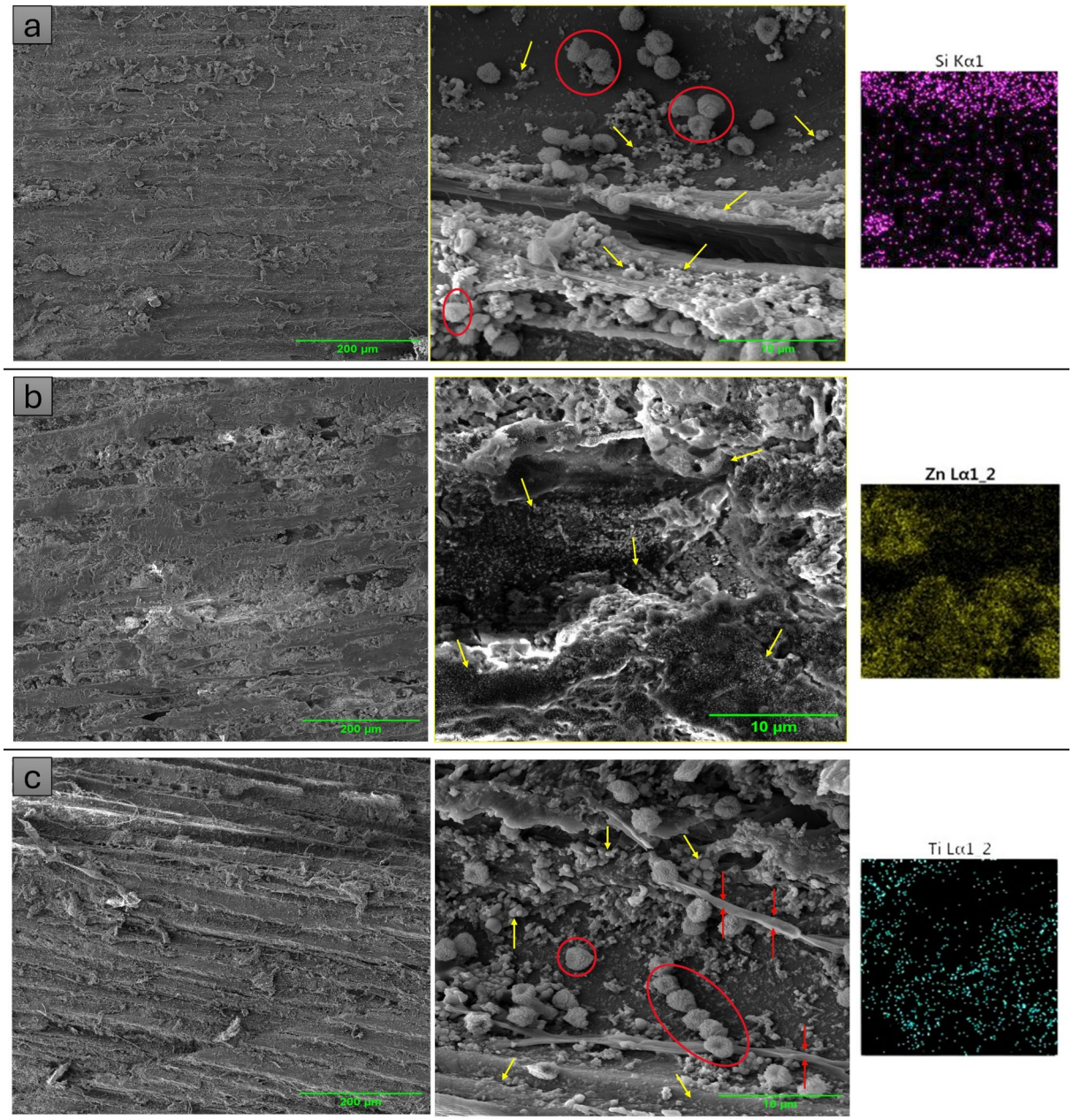

Figure 3 SEM image of high (left side), low (middle) resolution and distribution (right side) of coating samples exposed to blue stain fungi **a** Silicon dioxide (SiO_2), **b** Zinc oxide (ZnO), **c** Titanium dioxide (TiO_2).

and arrows), suggesting partial antifungal effectiveness, likely due to a surface barrier that did not completely seal the wood structure [18]. Elemental mapping confirms the presence of silicon particles on the surface. Figure 3b shows the ZnO-coated sample, where fungal structures are absent and the surface was densely covered with ZnO particles. The lack of visible pits suggests that the coating effectively blocked fungal entry and colonisation. Zinc particle distribution is confirmed through elemental mapping, indicating consistent surface coverage. In Fig. 3c, the TiO_2 coated sample shows limited fungal presence, less than in Control_B but more than ZnO, indicating moderate antifungal performance. This is likely influenced by particle agglomeration, as the surface shows denser clustering. Elemental mapping confirms the presence of titanium.

Previous study shows that nanoparticles such as ZnO, TiO_2 and SiO_2 can effectively penetrate and distribute within the wood matrix when their size is smaller than the wood's pore diameter (~ 10,000 nm) or bordered pit openings (400–600 nm) [21, 40]. These interactions are facilitated by the wood's high hydrophilicity, attributed to its abundance of hydroxyl groups, which enables strong hydrogen bonding with hydrophilic inorganic precursors [41], as confirmed by FTIR analysis in this study. This process transforms the wood surface from hydrophilic to hydrophobic, thereby enhancing its resistance to environmental and biological degradation [42, 43], as also demonstrated by contact angle measurements. Although SEM images show some particles agglomeration, which limits precise size measurement, the persistent presence of particles after fungal exposure suggests successful integration into the wood matrix [39] and supports their nanoscale dimensions [44]. Larger or loosely adhered particles would likely have detached during fungal colonisation. Overall, SEM analysis shows that ZnO-coated samples offer the most effective fungal resistance, TiO_2 provides moderate protection, and SiO_2 is the least effective. These results support the nanoscale behaviour and protective function of the oxide coatings, in line with established physicochemical mechanisms. Previous studies show that ZnO exhibits antibacterial properties in wood [19, 45].

Fourier transform infrared spectroscopy (FTIR)

The FTIR spectra of Fig. 4 reveal key differences and similarities among the samples, including uncoated and unexposed to blue stain (Control_A), uncoated but exposed to blue stain (Control_B), and coated samples (ZnO, SiO_2, TiO_2) exposed to blue stain. The functional group vibrations, including O – H, C – H, C = O, and C – O, as well as the oxide, reveal chemical transformations resulting from fungal activity and surface coating with nanoparticles. The O – H stretching band, observed between 3300–3346 cm^{-1}, appears at 3330 cm^{-1} in uncoated wood (Control_A) and shifts to 3340 cm^{-1} upon fungal exposure (Control_B), suggesting increased hydrogen bonding or formation of new hydroxyl groups due to polysaccharide degradation [46]. This band further shifts in coated samples to 3346 cm^{-1} (SiO_2), 3339 cm^{-1} (ZnO), and 3336 cm^{-1} (TiO_2), indicating that all coatings influence the wood's hydrogen bonding network, with SiO_2 showing the strongest interaction, likely due to hydrogen bonding or siloxane linkages. The C – H stretching region (2922–2929 cm^{-1} and 2851–2868 cm^{-1}) [47] representing methyl and methylene groups in lignin and cellulose, also shows subtle shifts. These bands appear at 2929 cm^{-1} and 2865 cm^{-1} in Control_A and shift slightly in Control_B to 2929 and 2868 cm^{-1}, reflecting fungal-induced structural changes. Coated samples

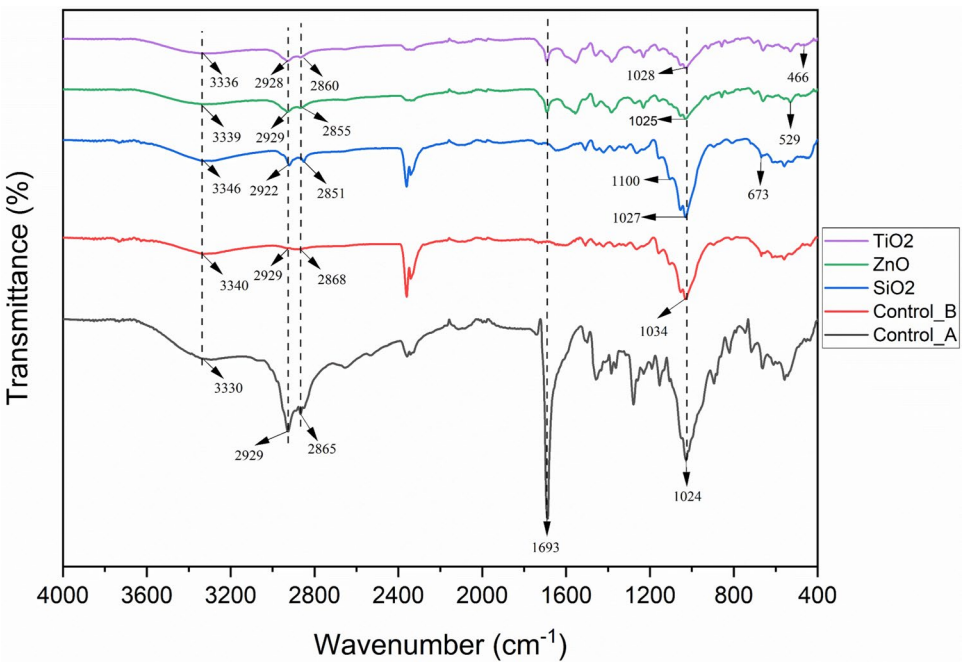

Figure 4 FTIR spectra of uncoated samples with and without exposure to blue stain and coated samples exposed to blue stain.

exhibit further downward shifts 2922/2851 cm^{-1} for SiO_2, 2929/2855 cm^{-1} for ZnO, and 2928/2860 cm^{-1} for TiO_2, suggesting that nanoparticle coatings influence the molecular environment, with SiO_2 again showing the most pronounced effect. The C = O stretching band at 1693 cm^{-1} remains consistent across all samples but may show increased intensity in stained wood due to oxidative lignin degradation and accumulation of carbonyl-rich metabolites [48]. The C – O stretching region, indicative of alcohols and polysaccharides, shifts from 1024 cm^{-1} in Control_A to 1034 cm^{-1} in Control_B, and 1027, 1025, and 1028 cm^{-1} in SiO_2, ZnO, and TiO_2 coated samples, respectively, reflecting fungal degradation and potential interactions between the coatings and the wood's carbohydrate components. Finally, the low-wavenumber peaks at 673, 529, and 466 cm^{-1} in SiO_2, ZnO, and TiO_2 coated samples, respectively, correspond to Si – O [49, 50], and Ti – O [51] vibrations. A prominent peak at 1100 cm^{-1} characteristic of Si – O – Si asymmetric stretching, confirming the formation of a silica network on the wood surface, with potential overlap from native wood C – O vibrations. These metal–oxygen peaks serve as definitive fingerprints of nanoparticle coatings, confirming successful surface treatment. They also help distinguish coated samples from uncoated controls and demonstrate the chemical integration of the coatings [52, 53]. The results of the FTIR spectra reveal that both fungal exposure and nanoparticle treatments induce measurable changes in the chemical structure of pine wood. Shifts in O – H,C – H, and C – O stretching bands confirm enzymatic degradation by fungi and molecular interactions with nanoparticle coatings. SiO_2 showed the most pronounced influence on hydrogen bonding and polysaccharide structure, while ZnO and TiO_2 also introduced distinct modifications without fully inhibiting lignin oxidation. Additionally, the presence of characteristic oxide vibrations confirmed the successful application of nanoparticle coatings. The FTIR result confirms that functional groups in wood support in situ nucleation and growth of oxides, leading to the formation of stable organic–inorganic hybrid composites [9, 18, 19]. The nanoparticles are anchored within the wood matrix by penetrating the micro- and mesopores of the cell wall, ensuring close interaction with wood polymers and enhancing resistance to fungal attack [18]. While XRD analysis will be pursued in future work to confirm crystalline oxide phases, the current results indicate that the nanoparticles remained embedded in the wood matrix after fungal exposure. These findings highlight the potential of ZnO, $SiO_2$and TiO_2 as protective treatments, with FTIR effectively capturing wood-coating-fungi interactions.

Durability and Wettability test of exposed and unexposed blue stain wood samples

Buchholz hardness was measured in fibre direction to assess how the wood's anisotropic nature affects its surface hardness, as shown in Fig. 5a. The analysis of Buchholz hardness reveals that the resistance of coated surfaces to plastic deformation was evaluated using the Buchholz hardness test under a load of 2 kg and a duration of 30 s. Control_A exhibited higher hardness both along (14.73 ± 3.68 μm) and across (12.85 ± 3.90 μm) the fibre direction compared to Control_B (12.86 ± 9.30 μm along and 10.12 ± 2.47 μm across), with a statistically significant reduction observed across the fibre ($p < 0.05$). Among the coated samples, TiO_2 demonstrated the highest resistance to plastic deformation (16.34 ± 3.77 μm along fibre), which was significantly higher than Control_B ($p < 0.05$). SiO_2 provided moderate, directionally consistent performance, whereas ZnO showed limited reinforcement, especially along the fibre (6.24 ± 2.29 μm); significantly lower than Control_B ($p < 0.05$), suggesting a less effective protective barrier in this configuration. Similarly, an investigation revealed that high concentrations of cellulose fibres affected the morphology, durability, and protective properties of wood paint, highlighting their impact on coating performance and the challenges of integration [54]. Another article examined the effects of ethylene oxide sterilisation. It accelerated ageing effects on the physical and mechanical properties of beech, elm, and oak wood, focusing on Buchholz hardness, surface hardness, durability, and dimensional stability [55]. Our study is the first to report nanoparticle coatings on wood surfaces, with a focus on Buchholz hardness. The results show that hardness varies with fibre orientation, affecting durability and resistance to indentation.

Young's modulus was measured to determine the elastic modulus, which highlights the effects of blue-stain exposure and subsequent oxide treatments on the mechanical rigidity of the wood, as shown in Fig. 5b. Control_A presented a higher value (707.82 ± 94.15 MPa) than Control_B (549.42 ± 40.04 MPa), with a statistically significant reduction observed due to fungal exposure ($p < 0.05$), confirming structural

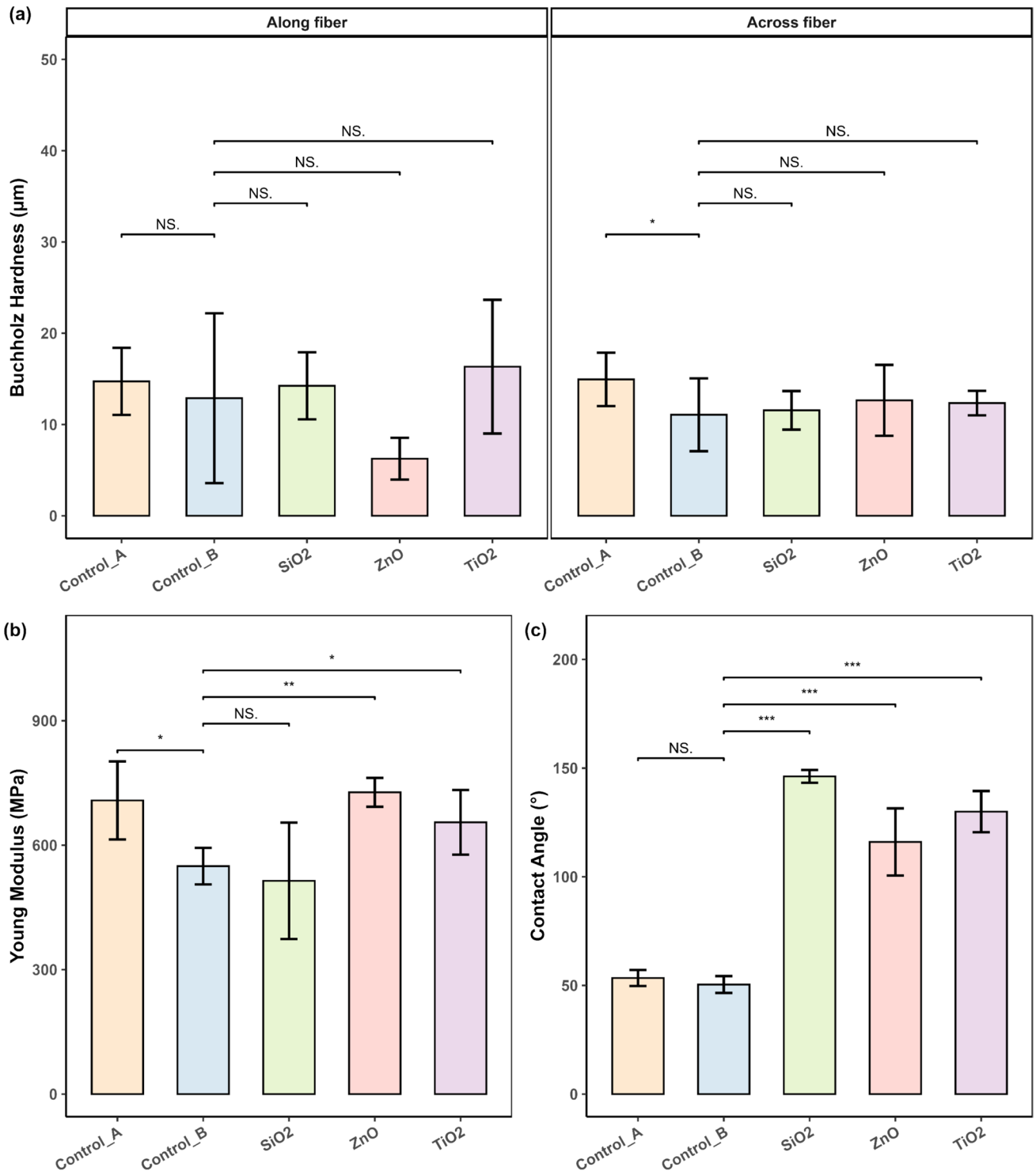

Figure 5 Mechanical and surface properties of wood under three conditions: uncoated without blue-stain exposure (Control_A), uncoated with blue-stain exposure (Control_B), and blue-stain exposed samples coated with SiO_2, ZnO, or TiO_2. **a** Buchholz hardness (left: along fibre, right: across fibre) and **b** Young's modulus were analysed using the Wilcoxon rank-sum test due to non-normal data distributions, while **c** contact angle was analysed using two-tailed Student's t-tests following a significant one-way ANOVA, after confirming normality. All bars represent mean ± standard deviation (SD); significance levels are indicated as $p < 0.05$ (*), $p < 0.01$ (**), $p < 0.001$ (***), and NS (not significant).

degradation. Treatment with ZnO restored and slightly improved rigidity (727.40 ± 38.21 MPa), significantly higher than Control_B ($p < 0.05$), followed by TiO_2 (655.46 ± 82.89 MPa, $p < 0.05$), both indicating successful mechanical stability. In contrast, SiO_2 demonstrated the lowest modulus (514.05 ± 120.29 MPa), indicating increased elasticity and reduced load-bearing capacity. The results clearly show that compare to blue-stain exposure significantly reduces wood stiffness, as seen in Control_B [27]. Treatments with ZnO and TiO_2 effectively restored or enhanced mechanical rigidity with statistical significance ($p < 0.05$), demonstrating their potential for structural reinforcement. ZnO showed the highest recovery, surpassing even uninfected wood. In contrast, SiO_2 was less effective, indicating limited improvement in mechanical performance. Additionally, previous research evaluated that fungal attack reduced wood stiffness and overall mechanical performance [27, 56, 57]. Our research proves that nanoparticle coating decreases the tendency for mechanical properties to deteriorate. Our study examined the effect of fungal attack on the stiffness and mechanical properties of wood. The results show that nanoparticle coatings help reduce the deterioration of these properties.

Wettability was assessed through contact angle measurements, which revealed significant improvements in surface hydrophobicity [58] following nanoparticle coating, as shown in Fig. 5c. Both controls were hydrophilic, with Control_A and Control_B displaying contact angles of 59.28 ± 3.17° and 55.61 ± 4.09°, respectively. In contrast, all coated surfaces exhibited enhanced water repellence, with SiO_2 achieving a superhydrophobic state (146.38 ± 2.94°) significantly higher than Control_B ($p < 0.001$). TiO_2 (129.96 ± 9.40°) and ZnO (116.04 ± 15.45°) also imparted considerable hydrophobicity, both statistically significant compared to Control_B ($p < 0.001$). Though SiO_2 was most effective in reducing wettability, TiO_2 offered a more balanced performance, enhancing surface hardness, restoring structural rigidity, and improving moisture resistance. The wettability analysis clearly distinguishes the effects of blue stain exposure and subsequent oxide treatments. Both Control_A and Control_B were hydrophilic, with lower contact angles indicating poor water resistance. Blue stain slightly reduced the hydrophobicity of the surface, as seen in Control_B. However, all nanoparticle coatings significantly improved water repellence. SiO_2 stood out with superhydrophobic behaviour, showing the highest contact angle, making it most effective at minimising wettability. TiO_2 and ZnO [58] also enhanced surface hydrophobicity but to a lesser extent. Notably, TiO_2 demonstrated a more balanced performance by improving water resistance and contributing to mechanical reinforcement. Figure S1 visually demonstrates that coatings can effectively alter wettability, thereby influencing the performance of wood. Similarly, a study found that heat coating reduced the surface wettability of blue-stained wood, as indicated by increased contact angles and decreased water absorption [59, 60]. These results highlight the potential of TiO_2 as a multifunctional surface treatment, while SiO_2 is ideal when maximum water repellence was desired.

The influence of surface roughness on wettability was examined through static water contact angle measurements across several samples. The uncoated Control_A surface exhibited an intrinsic contact angle of $\theta^\circ = 59.28^\circ$, serving as a smooth reference.

To evaluate the role of roughness, Wenzel's equation was applied:

$$\cos\theta = r \cdot \cos\theta^\circ \tag{1}$$

where θ is the apparent contact angle on the rough surface, θ° is the contact angle on a smooth surface, and r is the roughness factor.

For Control_B, the calculated roughness factor was $r = 1$, which aligns with Wenzel's model, where surface roughness enhances the material's inherent wettability. However, for the coated samples, SiO_2 ($r = -1.63$), TiO_2 ($r = -1.26$), and ZnO ($r = -0.89$), the roughness factors were negative, which is physically meaningless, as r must be greater than or equal to 1. These results from the coated samples suggest that Wenzel's model does not apply to these coated surfaces.

The failure of Wenzel's equation suggests a transition to the Cassie-Baxter regime, where water droplets rest partially on air pockets trapped within the surface texture rather than fully wetting the solid. The Cassie–Baxter equation describes this behaviour:

$$\cos\theta = f_s \cos\theta^\circ + \left(1 - f_s\right) \tag{2}$$

where f_s is the fraction of solid in contact with the liquid. Applying this model yielded $f_s = (SiO_2 = 3.74$, $TiO_2 = 3.35$ and $ZnO = 2.97)$. Although these values exceed physical bounds, they indicate that the surfaces are not fully wetted and instead behave as composite solid–air interfaces, consistent with superhydrophobic behaviour. These results demonstrate that increased

surface roughness, in combination with appropriate coatings, can significantly enhance water repellency, particularly when air becomes trapped beneath the droplet, as described by the Cassie-Baxter model.

From the perspective of surface roughness, Control_A, being uncoated and unexposed, exhibited a moderate contact angle (59.28°), representing a relatively smooth and clean surface. Control_B, exposed to blue stain fungi, showed a slightly lower angle (55.61°), suggesting increased surface roughness due to fungal attack, which can create micro-structural irregularities. In contrast, the coated samples (SiO_2, TiO_2, ZnO), despite also being exposed to fungi, exhibited significantly higher contact angles from Fig. 4c, indicating that the nanoparticle coatings introduced functional roughness that, in combination with low surface energy, promoted superhydrophobic or highly water-repellent behaviour. This increase in roughness was visibly confirmed by SEM images, which showed more textured and hierarchical surface structures on the coated samples compared to the smoother appearance of the controls.

Colour changes and image analysis of affected wood

The colour test was performed according to the CIELAB colour measurement system, where L* represents lightness, a* represents the green–red axis, and b* represents the blue-yellow axis. The following equation defines the colour difference:

$$\Delta E^* = \sqrt{(\Delta L^*)^2 + (\Delta a^*)^2 + (\Delta b^*)^2} \quad (3)$$

where ΔE^* is colour difference, L^* is lightness difference, a^* is the chroma change from green to red or in the other direction, b^* is the chroma change from blue to yellow or in the other direction.

ΔE represents the total colour difference and was calculated from the L, a, and b values before and after coating. It cannot be determined for "before exposure to blue stain" samples, as there is no change to measure. All results were compared to Control_A (uncoated and unexposed), which served as the reference for evaluating the impact of fungal exposure and nanoparticle treatments. From Table 1, it was observed that exposure to blue stain fungi resulted in a dramatic reduction in lightness (L^* dropped from 80.5 to 26.66 in Control_B) and a significant overall colour change ($\Delta E = 55.33$), confirming severe discolouration. The SiO2 coating best preserved the original appearance ($L^* = 69.07$, $\Delta E = 12.28$), exhibiting strong resistance to fungal darkening with only a slight blue hue. TiO_2 provided moderate protection ($L^* = 61.13$, $\Delta E = 19.56$), also showing a slight bluish tint. The ZnO coating, which showed the most significant deviation from Control_A ($L^* = 54.33$, $\Delta E = 33.4$), effectively prevented blue stain fungi, as no blue tint was observed. The colour change in the ZnO coating sample was due to the coating itself, not the fungus. Overall, coatings reduced the visual impact of fungal exposure compared to Control_A, with SiO_2 being the most colour-stable, TiO_2 offering balanced performance, and ZnO providing the strongest antifungal protection with noticeable colour alteration as visually observed in Fig. S2. Blue stain fungi primarily target the sapwood, causing discolouration with a blue or greyish tint by infecting the cell walls and disrupting the wood's natural appearance [56, 61]. Nanoparticle coatings, such as those made from SiO_2, ZnO, and TiO_2, enhance wood's resistance to blue stain fungi by preventing fungal colonisation, limiting moisture uptake, and preserving the wood's aesthetic quality [9, 62]. These coatings work through antifungal properties, surface modifications that reduce fungal attachment, and increased water repellence [58, 63]. The effectiveness of these coatings in preventing discolouration depends on factors like composition and conditions, with nanoparticle treatments improving colour stability.

Table 1 The colour changes of the uncoated with and without exposure to blue stain fungi and coated samples after exposure to the blue stain fungi

Sample	L*	a*	b*	ΔE
Control(A)	80.5	14.7	21.3	–
Control(B)	26.66	12.8	8.66	55.33
SiO_2	69.07	10.5	19.71	12.28
ZnO	54.33	31.13	34	33.4
TiO_2	61.13	12.66	19.46	19.56

The image processing analysis in Fig. 6 was performed using ImageJ software. The data included only samples exposed to blue stain fungi, both Coated and uncoated. The percentages were calculated based on the total and affected areas of each sample. The magnitude of these results lies in their potential implications for understanding the resistance or susceptibility of different materials (samples)

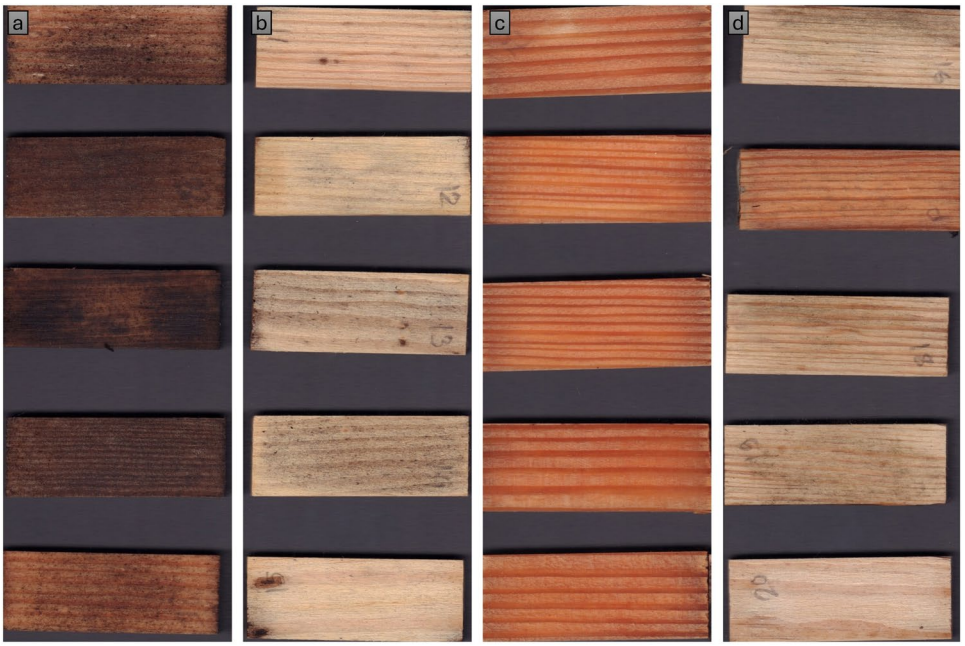

Figure 6 Image of exposed blue stain fungi samples: **a** uncoated (Control_B), **b** Silicon dioxide (SiO_2), **c** Zinc oxide (ZnO), **d** Titanium dioxide (TiO_2).

to the specific factor or condition that affects the area. For instance, the Control_B sample's high percentage of affected area (90.51%) suggests it is highly susceptible to the tested condition, making it less suitable for applications where durability or resistance is critical.

In contrast, the SiO_2 coated sample, with a significantly lower affected area percentage of 13.21%, along with ZnO and TiO_2, which have affected area percentages of 3.70% and 6.21%, respectively, demonstrates greater resistance. These materials were more desirable for use in environments where minimal impact or degradation was essential. ImageJ software was widely used to analyse fungal degradation on coated and uncoated materials [64]. Similarly, a previous study used ImageJ software to assess mould growth and blue stain discolouration on coated wood surfaces by analysing digital images, highlighting its effectiveness in evaluating fungal resistance and coating performance [65]. In our study, we developed a simple and objective method for assessing blue stain fungal growth on coated wood using ImageJ software. By analysing digital images to measure affected areas, we efficiently evaluated the spread of blue stain fungi. This approach provided a reliable visual and quantitative assessment of fungal colonisation, enabling us to compare the protective performance of different nanoparticle coatings. The results helped identify coatings that effectively limited fungal growth and preserved the wood's surface aesthetics.

Comparative analysis reveals that ZnO coatings provide the most effective antifungal protection, TiO_2 offers a balanced improvement in mechanical strength and hydrophobicity, while SiO_2 excels in preserving surface aesthetics and achieving hydrophobicity. SEM, FTIR, and ImageJ analyses confirm that all nanoparticles were successfully incorporated into the wood matrix nanocomposite hybrid material [29] and remained stable following fungal exposure. Although TiO_2 likely exists in an amorphous state due to the relatively low curing temperature, its performance remains noteworthy. Future research should investigate the effects of varying nanoparticle concentrations, confirm crystalline phases using XRD or Raman spectroscopy, and expand mechanical and physical testing. These insights could guide material selection for specific industrial applications, helping to optimise performance, longevity, aesthetics, and cost-effectiveness based on how different materials respond to the conditions they will encounter.

Conclusion

This research demonstrated the impact of low-concentration nanoparticle coatings on wood, showing significant improvements in hydrophobicity, mechanical

performance and resistance to blue-stain fungi. For the first time, we assessed the effects of these nanoparticle coatings on wood's Buchholz hardness and mechanical performance under fungal attack. Furthermore, the ImageJ based method developed in this study provided an efficient and objective way to evaluate and compare the effectiveness of coatings. Among the coatings tested, ZnO emerged as the most effective in providing fungal protection and mechanical strength, while SiO_2 enhanced moisture resistance, and TiO_2 offered a balanced performance. Overall, our results demonstrated that these coatings prevent fungal colonisation, reduce moisture absorption, and maintain the wood's aesthetic quality, thereby enhancing the performance quality of the nanocomposite in wood nanoparticles in construction, furniture, and outdoor applications.

Acknowledgements

The Internal Grant Agency for Individual Projects at Mendel University in Brno supported and funded this research. The specific project number associated with this support is IGA-FFWT-23-IP-026. We acknowledge CzechNanoLab Research Infrastructure supported by MEYS CR (LM2023051). The financial support of the Slovenian Research and Innovation Agency (ARIS) is highly appreciated in the frame of the project J7-50231 (GROWTH) and program P4-0015.

Author contributions

Dabosmita Paul: Writing – review & editing, Writing – original draft, Visualisation, Methodology, Investigation, Formal analysis, Data curation, Conceptualisation. Miha Humar: Writing – review & editing, Writing – original draft, Methodology, Visualisation, Validation. Daniela Tesařová: Writing – review & editing, Validation. Marko Petrič: Writing – review & editing, Validation Conceptualisation. Milan Gaff: Writing – review & editing.

Funding

Open access publishing supported by the institutions participating in the CzechELib Transformative Agreement.

Data and code availability

The datasets and code generated or analysed during the current study are not publicly available due to ongoing related work, but are available from the corresponding author upon reasonable request.

Declarations

Conflict of interest The authors declare that they have no known competing financial interests or personal relationships that could have appeared to influence the work reported in this paper.

Ethical approval Not applicable.

Supplementary Information The online version contains supplementary material available at https://doi.org/10.1007/s10853-025-11247-0.

References

[1] Xue M, Dai M, Li H et al (2024) Understanding the benefits and challenges of harvested wood products in response to climate change. Resour Conserv Recycl 209:107739. https://doi.org/10.1016/j.resconrec.2024.107739

[2] Siau JF (1984) Wood structure and chemical composition. Transport processes in wood. Springer, Berlin Heidelberg, pp 35–72

[3] Rowell RM (2005) Handbook of wood chemistry and wood composites. Taylor & Francis, Boca Raton, Fla

[4] Pettersen RC (1984) The chemical composition of wood. In: The chemistry of solid wood. american chemical society, pp 57–126

[5] Bardage S, Westin M, Fogarty HA, Trey S (2014) The effect of natural product treatment of southern yellow pine on fungi causing blue stain and mold. Int Biodeterior Biodegrad 86:54–59. https://doi.org/10.1016/j.ibiod.2013.09.001

[6] Humar M, Vek V, Buar B (2008) Properties of blue-stained wood. Drvna Ind 59(2):75–79

[7] Petrič M (2013) Surface modification of wood. Rev Adhes Adhes 1:216–247. https://doi.org/10.7569/RAA.2013.097308

[8] Chang H-T, Chang S-T (2002) Moisture excluding efficiency and dimensional stability of wood improved by acylation. Bioresour Technol 85:201–204. https://doi.org/10.1016/S0960-8524(02)00085-8

[9] Kanokwijitsilp T, Traiperm P, Osotchan T, Srikhirin T (2016) Development of abrasion resistance SiO_2 nanocomposite coating for teak wood. Prog Org Coat 93:118–126. https://doi.org/10.1016/j.porgcoat.2015.12.004

[10] Xie Y, Krause A, Mai C et al (2005) Weathering of wood modified with the N-methylol compound 1,3-dimethylol-4,5-dihydroxyethyleneurea. Polym Degrad Stab 89:189–199. https://doi.org/10.1016/j.polymdegradstab.2004.08.017

[11] Srinivas K, Pandey KK (2012) Effect of heat treatment on color changes, dimensional stability, and mechanical properties of wood. J Wood Chem Technol 32:304–316. https://doi.org/10.1080/02773813.2012.674170

[12] Jirouš-Rajković V, Miklečić J (2021) Enhancing weathering resistance of wood—a review. Polymers 13:1980. https://doi.org/10.3390/polym13121980

[13] Gérardin P (2016) New alternatives for wood preservation based on thermal and chemical modification of wood— a review. Ann For Sci 73:559–570. https://doi.org/10.1007/s13595-015-0531-4

[14] Yildiz S, Gezer ED, Yildiz UC (2006) Mechanical and chemical behavior of spruce wood modified by heat. Build Environ 41:1762–1766. https://doi.org/10.1016/j.buildenv.2005.07.017

[15] Xie Y, Fu Q, Wang Q et al (2013) Effects of chemical modification on the mechanical properties of wood. Eur J Wood Wood Prod 71:401–416. https://doi.org/10.1007/s00107-013-0693-4

[16] Davis K, Leavengood S, Morrell JJ (2021) Performance of exterior wood coatings in temperate climates. Coatings 11:325. https://doi.org/10.3390/coatings11030325

[17] Paul D, Gaff M, Tesařová D et al (2023) Recent advancements in nanotechnology application on wood and bamboo materials: A review. Nanotechnol Rev 12:20220528. https://doi.org/10.1515/ntrev-2022-0528

[18] Li J, Yu H, Sun Q et al (2010) Growth of TiO2 coating on wood surface using controlled hydrothermal method at low temperatures. Appl Surf Sci 256:5046–5050. https://doi.org/10.1016/j.apsusc.2010.03.053

[19] Dong Y, Yan Y, Ma H et al (2017) In-situ chemosynthesis of ZnO nanoparticles to endow wood with antibacterial and UV-resistance properties. J Mater Sci Technol 33:266–270. https://doi.org/10.1016/j.jmst.2016.03.018

[20] Keplinger T, Wittel FK, Rüggeberg M, Burgert I (2021) Wood derived cellulose scaffolds—processing and mechanics. Adv Mater 33:2001375. https://doi.org/10.1002/adma.202001375

[21] Petric M, Levanic J, Paul D (2023) Investigations of surface-treated wood by a micro-indentation approach: a short review and a case study. Bull Transilv Univ Brasov Ser II For Wood Ind Agric Food Eng. https://doi.org/10.31926/but.fwiafe.2023.16.65.3.13

[22] Kuroda A, Joly P, Shibata N et al (2008) An organic-inorganic hybrid composite as a coating agent. J Am Oil Chem Soc 85:549–553. https://doi.org/10.1007/s11746-008-1230-1

[23] Miyafuji H, Saka S (1997) Fire-resisting properties in several TiO2 wood-inorganic composites and their topochemistry. Wood Sci Technol 31:449–455. https://doi.org/10.1007/BF00702567

[24] Jiang F, Li T, Li Y et al (2018) Wood-based nanotechnologies toward sustainability. Adv Mater 30:1703453. https://doi.org/10.1002/adma.201703453

[25] Liu Y, Fu Y, Yu H, Liu Y (2013) Process of in situ forming well-aligned Zinc Oxide nanorod arrays on wood substrate using a two-step bottom-up method. J Colloid Interface Sci 407:116–121. https://doi.org/10.1016/j.jcis.2013.06.043

[26] Sofiaturizkiyah N, Priadi T (2023) The blue stain attack and its effect on the mechanical properties of five light-colour

woods. BIO Web Conf 77:01007. https://doi.org/10.1051/bioconf/20237701007

[27] Humar M, Viljem V, Bojan B (2008) Properties of blue-stained wood. Drv Ind 59:75–79

[28] Millers M, Magaznieks J, Gžibovska Z (2017) Blue stain development of scots pine (pinus sylvestris l) roundwood and its influencing factors, pp 120–126

[29] Dong X, Zhuo X, Wei J et al (2017) Wood-based nanocomposite derived by in situ formation of organic-inorganic hybrid polymer within wood via a sol-gel method. ACS Appl Mater Interfaces 9:9070–9078. https://doi.org/10.1021/acsami.7b01174

[30] Mishra R (2018) Materials chemistry and the futurist eco-friendly applications of nanocellulose: status and prospect. J Saudi Chem Soc. https://doi.org/10.1016/j.jscs.2018.02.005

[31] Setyawati MI, Tay CY, Leong DT (2015) Mechanistic investigation of the biological effects of SiO_2, TiO_2, and ZnO nanoparticles on intestinal cells. Small Weinh Bergstr Ger 11:3458–3468. https://doi.org/10.1002/smll.201403232

[32] Arpanaei A, Fu Q, Singh T (2024) Nanotechnology approaches towards biodeterioration-resistant wood: a review. J Bioresour Bioprod 9:3–26. https://doi.org/10.1016/j.jobab.2023.09.001

[33] Raspor P, Smole-Možina S, Podjavoršek J, et al (1995) ZIM: Collection of industrial microorganisms

[34] Schmidt O (2006) Wood cell wall degradation. Wood and tree fungi: biology, damage, protection, and use. Springer, Berlin, Heidelberg, pp 87–107

[35] Wickham H, François R, Henry L et al (2023) dplyr: a grammar of data manipulation. R package version 1(1):2

[36] Allaire JJ RStudio: Integrated Development Environment for R

[37] Chu BTT, Tobias G, Salzmann CG et al (2008) Fabrication of carbon-nanotube-reinforced glass–ceramic nanocomposites by ultrasonic in situ sol–gel processing. J Mater Chem 18:5344–5349. https://doi.org/10.1039/B809369E

[38] Wang Y-Y, Wang X-Q, Zhang B-Z et al (2024) SiO2 decorated wood nanocomposite with enhanced mechanical performance, flame and water resistance. Nano Mater Sci. https://doi.org/10.1016/j.nanoms.2024.09.005

[39] Wang B, Feng M, Zhan H (2014) Improvement of wood properties by impregnation with TiO_2 via ultrasonic-assisted sol–gel process. RSC Adv. https://doi.org/10.1039/C4RA04852K

[40] Kartal SN, Green F, Clausen CA (2009) Do the unique properties of nanometals affect leachability or efficacy against fungi and termites? Int Biodeterior Biodegrad 63:490–495. https://doi.org/10.1016/j.ibiod.2009.01.007

[41] Hübert T, Unger B, Bücker M (2010) Sol–gel derived TiO2 wood composites. J Sol-Gel Sci Technol 53:384–389. https://doi.org/10.1007/s10971-009-2107-y

[42] Tshabalala MA, Sung L-P (2007) Wood surface modification by in-situ sol-gel deposition of hybrid inorganic–organic thin films. J Coat Technol Res 4:483–490. https://doi.org/10.1007/s11998-007-9033-0

[43] Tshabalala MA, Gangstad JE (2003) Accelerated weathering of wood surfaces coated with multifunctional alkoxysilanes by sol-gel deposition. J Coat Technol 75:37–43. https://doi.org/10.1007/BF02730098

[44] Kim T, Lee J (2023) Silicon nanoparticles: fabrication, characterization, application and perspectives. Micro Nano Syst Lett 11:18. https://doi.org/10.1186/s40486-023-00184-9

[45] Bazant P, Munster L, Machovsky M et al (2014) Wood flour modified by hierarchical Ag/ZnO as potential filler for wood–plastic composites with enhanced surface antibacterial performance. Ind Crops Prod 62:179–187. https://doi.org/10.1016/j.indcrop.2014.08.028

[46] Poletto M, Zattera AJ, Santana RMC (2012) Structural differences between wood species: evidence from chemical composition, FTIR spectroscopy, and thermogravimetric analysis. J Appl Polym Sci 126:E337–E344. https://doi.org/10.1002/app.36991

[47] Russo C, Stanzione F, Tregrossi A, Ciajolo A (2014) Infrared spectroscopy of some carbon-based materials relevant in combustion: qualitative and quantitative analysis of hydrogen. Carbon 74:127–138. https://doi.org/10.1016/j.carbon.2014.03.014

[48] Shinozaki A, Arima K, Morita M et al (2003) FTIR-ATR evaluation of organic contaminant cleaning methods for SiO_2 surfaces. Anal Sci 19:1557–1559. https://doi.org/10.2116/analsci.19.1557

[49] Hirata T (1997) Evolution of the infra-red vibrational modes upon thermal oxidation of Si single crystals. J Phys Chem Solids 58:1497–1501. https://doi.org/10.1016/S0022-3697(97)00179-0

[50] Yao Q, Wang C, Fan B et al (2016) One-step solvothermal deposition of ZnO nanorod arrays on a wood surface for robust superamphiphobic performance and superior ultraviolet resistance. Sci Rep 6:35505. https://doi.org/10.1038/srep35505

[51] Sun Q, Lu Y, Liu Y (2011) Growth of hydrophobic TiO2 on wood surface using a hydrothermal method. J Mater Sci 46:7706–7712. https://doi.org/10.1007/s10853-011-5750-y

[52] Wang S, Liu C, Liu G et al (2011) Fabrication of superhydrophobic wood surface by a sol–gel process. Appl Surf Sci 258:806–810. https://doi.org/10.1016/j.apsusc.2011.08.100

[53] Xing D, Zhang Y, Hu J, Yao L (2020) Highly hydrophobic and self-cleaning heat-treated *Larix* spp. prepared by TiO_2 and ZnO particles onto wood surface. Coatings 10:986. https://doi.org/10.3390/coatings10100986

[54] Calovi M, Rossi S (2023) Impact of high concentrations of cellulose fibers on the morphology, durability and protective properties of wood paint. Coatings 13:721. https://doi.org/10.3390/coatings13040721

[55] Effect of ethylene oxide sterilization and accelerated ageing on the physical and mechanical properties of beech, oak, and elm wood: Part 1: BioResources. Accessed 20 Jan 2025

[56] Nurul S, Trisna P (2023) The Blue Stain Attack and Its Effect on The Mechanical Properties of Five Light-Colour Woods. BIO Web Conf

[57] Millers M (2017) Blue stain development of scots pine (pinus sylvestris l) roundwood and its influencing factors. Res Rural Dev 1:120–126

[58] Weththimuni ML, Capsoni D, Malagodi M (2019) Licchelli M Improving Wood Resistance to Decay by Nanostructured ZnO-Based Treatments. J Nanomater 1:6715756

[59] Yu LL, Tang ZZ, Cao JZ, Yan L (2010) Properties of blue-stain masson pine after compression and thermal modification. Adv Mater Res 160–162:1199–1204. https://doi.org/10.4028/www.scientific.net/AMR.160-162.1199

[60] Wu Y, Wu X, Yang F et al (2020) Effect of Thermal Modification on the Nano-Mechanical Properties of the Wood Cell Wall and Waterborne Polyacrylic Coating. Forests 11:1247. https://doi.org/10.3390/f11121247

[61] Yin H, Ringman R, Moghaddam MS et al (2023) Susceptibility of surface-modified superhydrophobic wood and acetylated wood to mold and blue stain fungi. Prog Org Coat 182:107628. https://doi.org/10.1016/j.porgcoat.2023.107628

[62] Harandi D, Ahmadi H, Mohammadi Achachluei M (2016) Comparison of TiO2 and ZnO nanoparticles for the improvement of consolidated wood with polyvinyl butyral against white rot. Int Biodeterior Biodegrad 108:142–148. https://doi.org/10.1016/j.ibiod.2015.12.017

[63] Nosáľ E, Reinprecht L (2017) Anti-bacterial and anti-mold efficiency of ZnO nanoparticles present in melamine-laminated surfaces of particleboards. BioResources 12:7255–7267. https://doi.org/10.15376/biores.12.4.7255-7267

[64] Yonni F, Moreira MT, Fasoli H et al (2004) Simple and easy method for the determination of fungal growth and decolourative capacity in solid media. Int Biodeterior Biodegrad 54:283–287. https://doi.org/10.1016/j.ibiod.2004.03.017

[65] Van den Bulcke J, Van Acker J, Stevens M (2005) Image processing as a tool for assessment and analysis of blue stain discolouration of coated wood. Int Biodeterior Biodegrad 56:178–187. https://doi.org/10.1016/j.ibiod.2005.07.004